Implementation Quasi Z-Source Inverter for PV Applications Based on Finite Control Set-Model Predictive Control

Mohamed A. Ismeil*,**‡, Abualkasim Bakeer*, Mohamed Orabi*

*APEARC, Faculty of Engineering, Aswan University, Aswan 81542, Egypt

**Electrical Engineering Department, Faculty of Engineering, South Valley University, Qena 83523, Egypt

(melzanaty@apearc.aswu.edu.eg,abualkasim.bakeer@aswu.edu.eg, morabi@apearc.aswu.edu.eg)

‡Corresponding Author; Mohamed A. Ismeil, Electrical Engineering Department, Faculty of Engineering, South Valley University, Qena 83523, Egypt, Tel: +20 96 533 9479, Fax: +20 96 533 9479, melzanaty@apearc.aswu.edu.eg

Received: xx.xx.xxxx Accepted:xx.xx.xxxx

Abstract- This paper presents a model predictive control with a class of finite control set to harvest the maximum possible amount of energy from the Photovoltaic (PV) system as a renewable energy resource. The utilized topology is based on the quasi Z-Source Inverter due to its clear merits such as the higher reliability as well as the bucking-boosting functionality. The algorithm of Maximum Power Point Tracking (MPPT) generates the reference values for the current in an inductor that is the Influential factor in selecting an action state of shoot-through that adjusts the inverter to operate at Maximum Power Point (MPP). Then, the obtained power from PV modules is transferred to the standalone RL load over current mode control. Here, sensor-less technique is used to observe the inductor current to decrease the cost and complexity of the control design. The validity of the proposed technique is proven with the detailed theoretical analysis. The simulation results are introduced based on the MATLAB software package. Also, the proposed controller has been experimentally demonstrated on a laboratory set-up using TMS320F28335 series Digital Signal Processors (DSP).

Keywords Photovoltaic (PV) System; quasi Z-source Inverter (qZSI); Finite Control Set- Model Predictive Control (FCS-MPC)..

1. Introduction

Actually, the non-renewable energy resources such as fuel fossil, natural gas; etc. have a restricted quantity in overall the world. With the near future time, these resources of energy will die out for huge consumption versus the limited offered amount in the world. Therefore, the world will face a problem in economizing the necessary energy to fulfil the requirements of life. Consequently, it moves into utilizing the other renewable energy resources e.g. photovoltaic systems, wind turbines, tide energy, biomass energy, and hydro-electrical power. Renewable energy is really considered a friendly energy resource for the environment as less pollution and noise. With the advanced technology, the reduction of the cost for PV systems is achieved to increase their annual installed capacity up to 60 % from 2004 to 2009, and 80% in 2011[1]. The output voltage of the PV system is small and not sufficient to the level of load voltage as well as it has a DC value; where most of the loads have alternating power necessity. For the last decades, the voltage source inverter (VSI) and current source inverter (CSI) were the basic prevalent inverters. However, VSI has only the bucking mode for the input voltage, whereas CSI has only the boosting feature. Consequently, an extra stage before these inverters may be required. As a result of increasing the number of components, the costs will increase as well as efficiency [2].

The first model for Z-Source Inverter (ZSI) was introduced in the application of power electronics in 2002 to solve the abovementioned limitations of the conventional inverters; as shown in Fig. 1(a) [3,4]. Within the simple description, the general configuration of this novel family is demonstrated on employing two inductors and two capacitors within X-shape relevance. A diode is coupled in the front connection of this combination which is naturally turned on or

off according to the switching states of the converter. Then, a common inversion stage either single or three-phases is cascaded to invert the pulsate boosted voltage V_{dc}. ZSI family has a unique feature which is the buck and boost functionality. The voltage fed ZSI boosts the input voltage by utilizing the shoot-through (ST) during the zero state without modifying the other traditional six active states. Despite the advantages provided by ZSI, it also has some defects, including high inrush current, which has been overcome in [5]. A quazi Z-Source Inverter (qZSI) shown in Fig. 2(b) is a model developed from the traditional ZSI and has provided many advantages including decreasing the voltage stress at capacitors and switches, in addition, the input current has Continuous Conduction Mode (CCM) [6].

The pulsate DC boosted voltage and AC side (output current or output voltage) can be regulated by two signals the first one is duty cycle shoot-through (D) and the second is modulation index (M). Because of the limitation between M and D two-stage control is used for both standalone and grid in [7]. Moreover, it makes the overall control system complex and the response not fast. It is worth to mention that, the integration between D and M makes the increase of D decrease M where M=1-D and leads to an increase of THD. Furthermore, qZSI has Right Half-Plane Zero (RHPZ) which it decreases the response of the closed-loop system's dynamic performance. These factors make the system to be challengeable in designing the control system [8].

Today, Predictive Control has become a promising model in the applications of power electronics especially the class of Model Predictive Control (MPC). MPC offers many characteristics for converters control compared to the conventional PWM control methods; the predominant ones are [9, 10]:

- ✓ Easy to implement with the new micro-controller.
- ✓ There are no problems with the nonlinear constraint
- ✓ Several control targets can be achieved in a single control law, and
- ✓ The fast dynamic response towards the reference points.

In the traditional control such as PI controller, each control variable should have its compensation transfer function, thus, a number of control loops may be used which further complicate the overall control. However, in MPC all control variables are compared to its references values and put in only one cost function. From this point on Several control targets can be achieved in a single cost function. Two classes for MPC are used with power converters which are Continuous Control Set- MPC (CCS-MPC) and Finite Control Set- MPC (FCS-MPC) [11]. The main difference among them is that CCS-MPC requires a modulator stage to perform the control action; consequently, with the carrier frequency, the switching frequency remains constant. On the other hand, FCS-MPC does not require any type of modulators where the control decision is directly applied to the converter switches with a non-periodic fixed frequency. When it is mentioned about FCS-MPC, the concept of cost or objective function is mainly raised due to its key role in choosing the future switching state of the converter. The cost function contains the minimization of each absolute error between predict value and reference value multiply by a constant value called weight factor. The weight factors are selected to reflect the weightiness of each term. This constant has a direct effect to the system's response to load change [12].

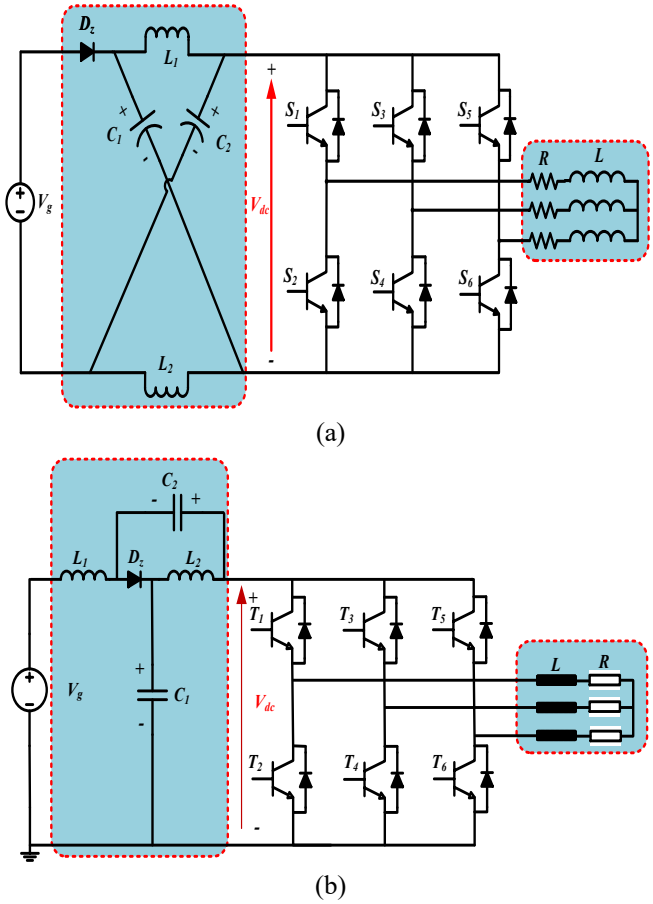

Fig. 1: a) Configuration of Z-Source Inverter b) Configuration of quasi Z-Source inverter.

The qZSI based on MPC for PV application is presented in a few research papers [13-15]. The work presented by [13] MPC is using to control only output AC current for Z-Source inverter, in addition, MPPT is achieved by an incremental conductance method. However, in [14] MPC is applied on qZSI to control the output AC currents, voltage on capacitor, and DC inductor current. In addition, in [14] limited simulation results based on MPC is presented with input voltage DC not PV as it mentioned in the title. In [15] ZSI is presented as a single stage to interphase between PV and grid using MPPT based on MPC, however, another PWM control is used to controlling the AC side only which makes the overall system very slow. Furthermore, in [15], the effect of unbalanced currents is ignored.

This paper provides a comprehensive cost function contain the output currents and inductor current without inductor current sensor. The observer term of inductor current improves the overall performance of the system compared to previous work. Besides, the total cost and size will decrease.

The objective of this paper is to use the Model Predictive Control (MPC) as a dominant control scheme incorporating with the attractive circuit of quasi-ZSI as an advanced topology in ZSI family; to track the maximum value of power from the PV system. qZSI needs a more complex design for the algorithm of FCS-MPC because of the unique state which is ST compared to VSI. The methodology to involve the shoot-through that is responsible for extracting MPP is stated here. Besides, it is the first time to use this controller experimentally with this family of inverters for the PV implementation. For a clear view of the contribution of this paper, it will be structured as the following: the system configuration for both PV modules and qZSI operation is briefly discussed in Section II. Then, the proposed controller is introduced in details within Section III. The simulation results are obtained based on the MATLAB software and introduced in Section IV. The proposed algorithm technique is validated vai experimental in Section V. Finally, in Section VI the conclusion is recorded.

2. System Under Investigation

2.1. PV Module

The energy from the PV cell is generated by failing the sunlight into its surface. The DC output voltage of the PV modules is not abundant to supply most electrical devices. Through connecting series and parallel of PV cells, the string is constructed. Connection of more than one strings together either series or parallel results the PV module.

The efficiency is improved if the peak power point of the module is extracted at all the environmental conditions. Several techniques for MPP of PV are introduced for this purpose as listed in [16-20]. The most effective techniques in MPPT include Perturb and Observe (P&O), Incremental Conductance (INC), and Fractional Open Circuit Voltage (FOCV). FCS-MPC was used to enhance MPPT for the fast dynamics in tracking the peak point of PV power under fast solar irradiation variation. In [21] an optimized scheme for MPPT is implemented in large-scale PV power conversion.

2.2. PV Module Quasi Z-Source Inverter Operation

When it is mentioned about Z-Source converter, the notion of shoot-through (ST) strongly appears as an extra state more than the conventional states of PWM converters. ST is selected to be a part of the zero state without effecting on the active states to avoid destroying the sinusoidal shape of the output voltage. In addition, the active state for the inverter which it delivers power to the load or grid is non shoot-through state and its schematic is shown in Fig. 2 b. however the equivalent circuit at load side is shown in Fig. 2 c.

3. Proposed Control Strategy

The main aim of this paper is to use the FCS-MPC approach for extracting the maximum power from PV modules based on qZSI as a significant topology of ZSI category. Generally, the Predictive Control is a straight-forward concept that extracts the future values and it compared with the reference value based on different switches states over a definite time horizon. The time horizon is being at least for one step forward. However, multiple steps horizon lead to more tracking for the reference values of variables regardless the outer disturbance; it has larger calculations burden; so, the high efficient processor is used to solve the optimization criterion and obtain the optimized switching state. The discrete model is used to predict the future values of variables. This model may be varied with operating modes of the converter. It is usually based on using the differential equations for inductor voltage and capacitor current; where they are the well-known utilized elements for most converters.

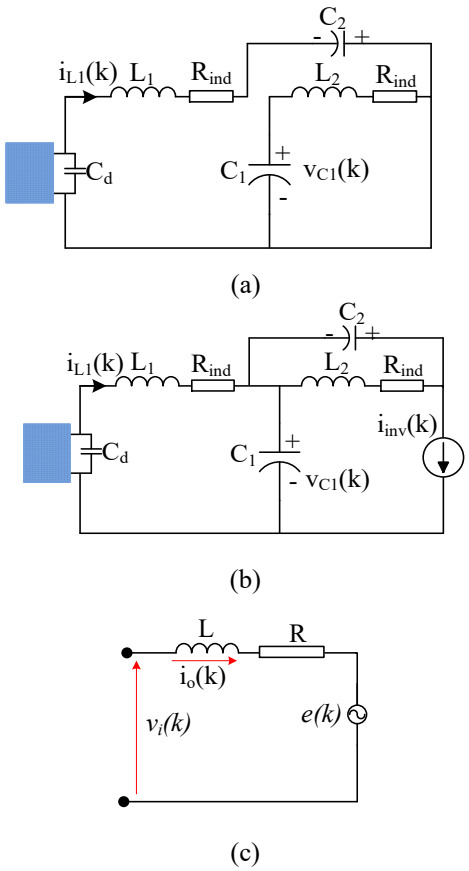

Fig. 2: an equivalent circuit for qZSI: a) non-shoot through case b) shoot through. and c) equivalent circuit of the load side

After that, these differential equations are converted into discrete terms of the sampling time by employing the mathematical theories. Basically, a converter that has a switching nature has different states which create active and zero states; where every switch has two states either ON or OFF. The probability of the states increases as the switches number increases in the converter schematic; this leads to the calculations delay and the control action is extremely affected. However, the rapid speed of recent digital platforms such as DSP, FPGA, etc. minimizes the influence of this shortage [22].

Figure 3 shows an example for the way that the Predictive Control follows to get an optimal value closed to the reference point of the variable, here is the inductor current as an example. Assuming the circuit of the inductor has only one switch; so, the inductor current has two future values which

are i_{L0} (k+1) and i_{L1} (k+1) when the switch is turned off and turned on respectively. These future values are computed based on converter modelling. The absolute error between the future current and the reference current at turning on the switch is E_1, while at turning off the switch is E_0. As shown in Fig. 3, E_1 has a smaller value than E_0. Consequently, for the converter, the optimized state in the next sampling time will be at turning on the switch of the converter. With the same above principle, the optimized state is selected based on the minimization of cost function if there are more than two states. Consequently, it's very important to set accurate modelling for the controlled items.

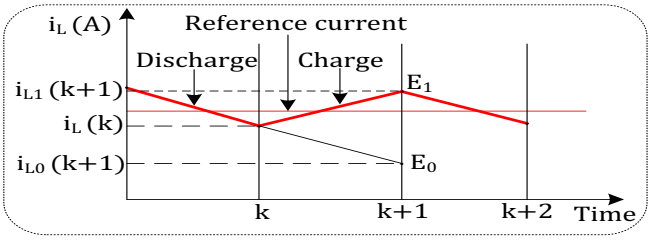

Fig. 3: Schematic diagram to show how FCS-MPC tracks the set point of control term.

3.1. Maximum Power Point Tracking Technique (MPPT)

Here, PV module is the input source of the power for the RL load as shown in Fig. 4. First of all, the P&O is chosen as MPP technique for its simplicity in the implementation of the experimental setup compared to other MPP techniques. at the instant (k) the for PV current and voltage are the two inputs for MPP algorithm. For qZSI, the only control input that regulates the converter to operate at the peak point of PV power is the shoot-through state. Fundamentally, the key factor in selecting the ST state is the inductor current, where it has only two prediction values as explained later. Thus, the output of the MPP algorithm will be the reference inductor current. The algorithm of MPP is updated every sampling time.

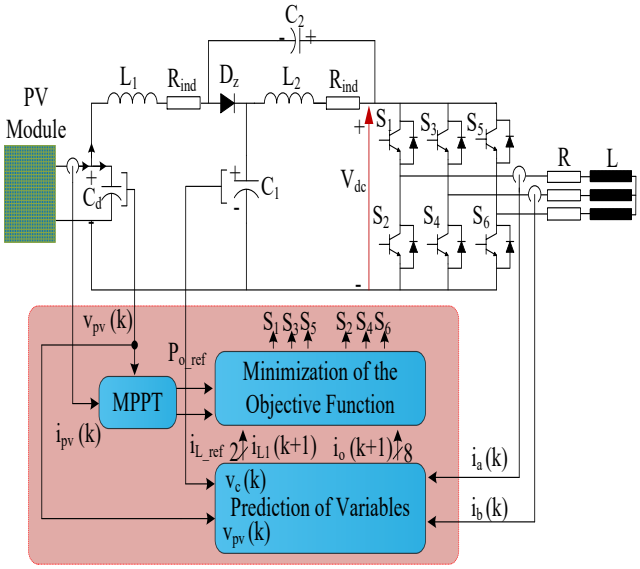

Fig. 4: Total schematic of the proposed system control based on MPC.

The difference between the current power and the previous one at an instant $(k-1)$ gives an indication for the direction of the PV power. Also, the change of the voltage is calculated by subtracting the current PV voltage from the previously stored one. According to the sign of (ΔP) and (ΔV); the decision of the algorithm is decided as follows: If (ΔP) and (ΔV) have a positive sign, this means that the algorithm should be tracked in the direction of increasing the power by increment the inductor reference current than the previous value by the magnitude of (δ); in addition, the maximum power point of the PV system can be obtained by decreasing the reference current using the control value (δ).

3.2. Discrete Model of the Load Current

The output AC currents are measured as feedback signals to the FCS-MPC. In the proposed system, symmetrical RL load is utilized; so the currents in two phases only are sensed instead of the three phases to reduce the number of sensors without affecting the control performance. These measured currents are mathematically transformed into the rotational coordinates (α,β) according to the prevalent Clark Transformation. The vector of the load voltage (V_i) of qZSI across the load terminals depends on the connection of inverter switches as:

$$V_i(k) = \frac{2}{3}V_{dc}(S_a + aS_b + a^2S_c) \quad (1)$$

where, $i \in \{0 - 7\}$, V_{dc} is the pulsated DC link voltage, S_a, S_b, S_c are gating signals for phase *a, b,* and *c* respectively (either 0 or 1 for upper switches and it is complementary for lower switches) the current control mode is used to control the output AC currents as the assumption that the RL load is a three phases machine controlled by the stator current. From Fig. 2 (c) the voltage across the inductor of the load can be given as:

$$L.\frac{di_o(k)}{dt} = V_i(k) - R.i_o(k) - e(k) \quad (2)$$

where, $e(k)$ is grid voltage and it equal zero as the load is RL and no grid connection.
The above equation can be approximated according to the Euler forward step method as:

$$\frac{di_o(k)}{dt} = \frac{1}{T_s}(i_o(k+1) - i_o(k)) \quad (3)$$

Therefore, the predict equation of output current $i_o(k+1)$ can be expressed as:

$$i_o(k+1) = \frac{1}{L+R.T_s}\left(T_s\left(V_i(k+1) - e(k+1)\right) + L.i_o(k)\right) \quad (4)$$

where, $V_i(k+1), T_s$, R and L are the inverter output voltage during each switching state.

The inverter AC output voltage at each state is listed in TABLE 1. the last state V_7 is corresponding of shoot-through state and the action in this state is selected to be all switches ON to decrease the conduction losses in power topology.
The setpoint of the peak phase current can be computed using the PV power with the assumption for full efficiency of the system as:

$$i_{o\_ref} = \sqrt{\frac{2.i_{pv}(k).v_{pv}(k)}{3.R}} \quad (5)$$

The reference current in the next state *(k+1)* is assumed extremely has the same value of one at (*k*) instant for small sampling time .both the predictive value for reference and actual load current are converted to coordinates (*α,β*).
The proposed cost function for the load current is expressed as:

$$g_{io}(i) = \left|i_{\alpha\_ref}(k+1) - i_{\alpha\_o}(k+1)\right| + \left|i_{\beta\_ref}(k+1) - i_{\beta\_o}(k+1)\right| \quad (6)$$

Table 1. AC output voltage of qZSI at each switching state.

AC Output Voltage V_i	S_1	S_3	S_5	S_2	S_4	S_6
$V_0 = 0$	OFF	OFF	OFF	ON	ON	ON
	ON	ON	ON	OFF	OFF	OFF
$V_1 = \frac{2}{3}.V_{dc}$	ON	OFF	OFF	OFF	ON	ON
$V_2 = \frac{1}{3}.V_{dc} + j.\frac{\sqrt{3}}{3}.V_{dc}$	ON	ON	OFF	OFF	OFF	ON
$V_3 = -\frac{1}{3}.V_{dc} + j.\frac{\sqrt{3}}{3}.V_{dc}$	OFF	ON	OFF	ON	OFF	ON
$V_4 = -\frac{2}{3}.V_{dc}$	OFF	ON	ON	ON	OFF	OFF
$V_5 = -\frac{1}{3}.V_{dc} - j.\frac{\sqrt{3}}{3}.V_{dc}$	OFF	OFF	ON	ON	ON	OFF
$V_6 = \frac{1}{3}.V_{dc} - j.\frac{\sqrt{3}}{3}.V_{dc}$	ON	OFF	ON	OFF	ON	OFF
$V_7 = 0$	ON	ON	ON	ON	ON	ON

3.3. Discrete Modelling for the DC Current in the Inductor of qZSI Network

The shoot-through case can be detected by the value of the inductor. In the proposed algorithm, it will not be sensed but its value will be defined through estimation methodology as described later. Although, qZSI has six active states, null state, and zero state; the inductor current has only two future values according to the next case:

A. The case of Non shoot-through State

$$i_{L_1}(k+1) = \frac{1}{L_1 + R_{ind}.T_s}\left(T_s.(v_{pv}(k) - v_{C_1}(k)) + L_1.i_{L_1}(k)\right) \quad (7)$$

B. The case of shoot-through State

$$i_{L_1}(k+1) = \frac{1}{L_1 + R_{ind}.T_s}\left(T_s.v_{C_1}(k) + L_1.i_{L_1}(k)\right) \quad (8)$$

where, L_1 is the inductance of the inductor, R_{ind} is the stray resistance of the inductor, $v_{C1}(k)$ is the capacitor voltage, and $i_{L_1}(k)$ is the inductor L_1 current at (k) instant. An important note is that the modelling for the capacitor voltage is not stated here because it is not being under controlled. However, if a grid connection for the proposed system is the objective; the capacitor voltage should be ensured fixed at a defined point to avoid increasing the value of voltage stress on the switched devices. For the inductor current, the proposed cost function will be given as:

$$g_{iL}(i) = \lambda_{iL}\left|i_{L\_ref}(k+1) - i_{L1}(k+1)\right| \quad (9)$$

where, λ_{iL} is the weighting factor for the inductor current and $i_{L\_ref}(k+1)$ is the reference current resulted from the P&O algorithm.

Cost plays a key part in designing the control for any system. If the control system performance is not affected by removing a used sensor, it will be a great improvement in the design. Reducing the number of sensors will save also the footprint and the size of the implementation for the control system. The inductor current here will not be sensed as mentioned before. Each of the optimized state of the switching at the previous state $(k-1)$, the capacitor voltage during this state $V_c(k-1)$, and the estimated inductor current in this state $i_{L_1}(k-1)$ will be stored. They are updated at every sampling time with the new values at the (k) state. If the previous optimized state was during the non shoot-through case, the value inductor current at (k) instant can be estimated from:

$$i_{L_1}(k) = \frac{1}{L_1 + R_{ind}.T_s}\left(T_s.(v_{pv}(k-1) - v_{C_1}(k-1)) + L_1.i_{L_1}(k-1)\right) \quad (10)$$

On the other hand, if the optimized state was during the shoot-through case; yields:

$$i_{L_1}(k) = \frac{1}{L_1 + R_{ind}.T_s}\left(T_s.v_{C_1}(k-1) + L_1.i_{L_1}(k-1)\right) \quad (11)$$

Equations (10) and (11) give the methodology to estimate the inductor current, for more illustration a diagram is sketched in Fig. 5. However, in Fig. 6. the flow chart of the proposed algorithm strategy is shown.

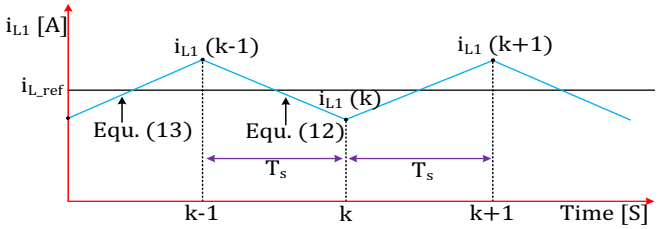

Fig. 5: Methodology of inductor current estimation.

The complete cost function of the proposed system will be as:

$$g(i) = \left|i_{\alpha\_ref}(k+1) - i_{\alpha\_o}(k+1)\right| + \left|i_{\beta\_ref}(k+1) - i_{\beta\_o}(k+1)\right| + \lambda_{iL}\left|i_{L\_ref}(k+1) - i_{L1}(k+1)\right| \quad (12)$$

4. Simulation Validation

Simulation under MATLAB/SIMULINK® software has been done to prove the achievability of the proposed control. The qZSI network has two inductors $L_1 = L_2$ with high inductance value of 6 mH to work in Discontinuous Conduction Mode (DCM) and each one has internal resistance R_{ind} equal 500 mΩ, two capacitors $C_1 = C_2$ with a value of 470

μF. the load is R-L with resistance 24 Ω /phase and inductance 74 mH/phase. The sampling time used is 90 µSec.

Furthermore, the line frequency of the AC side is set to be 50 Hz. The entire used components in this work are selected according to the available ones in the laboratory to be used in the experimental evaluation.

For the under-tested PV module, the BP solar model in MATLAB/SIMULINK library is used; but, their parameters are adjusted to coincide with the actual measurements for PV curve of the two utilized modules in the laboratory as shown in Fig. 7a and Fig. 7b.

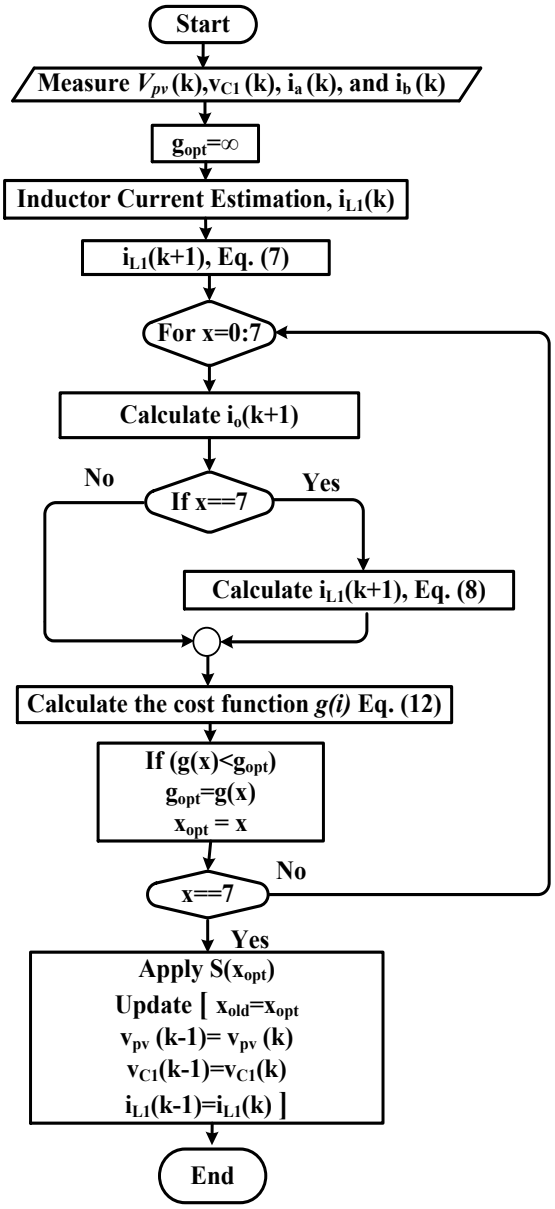

Fig. 6: Flow chart of the proposed control algorithm.

As shown in Fig. 7a and Fig. 7b, the maximum available power from the two modules is 110 W and 87 W respectively. MPP is roughly obtained at the same terminal voltage of the two modules at 17.5 V. This is an important factor that should be tested here because the two modules will be connected in parallel. Another issue is the investigation of robustness for the proposed controller; generally, MPC is mainly based on the actual parameters of system elements; so, changing the load is not an effective way to be applied here. Also for the available practical evaluation, it is not easy to make a variation in the irradiation level of the PV module. Consequently, the methodology is being through connecting a module in parallel with the main one as a step change point [23]. At this case, the controller should track the power of the two modules and extract it. However, FCS-MPC has the demerit of variable switching frequency; it can be solved through extra term added in the objective function to control the switching frequency. Generally, the maximum switching frequency of the system equals to half of the sampling frequency.

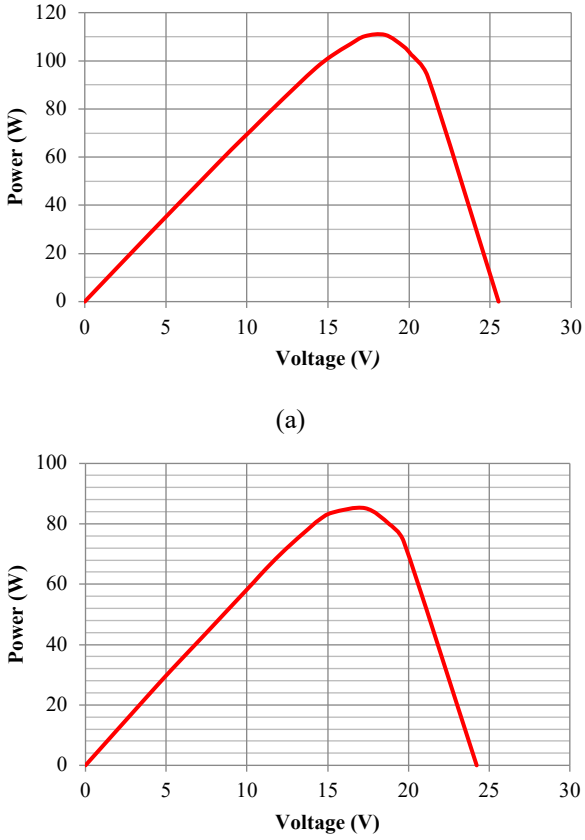

Fig. 7: Practical PV curves for PV modules: a) the first module, and b) the second module.

The simulation results of the proposed controller at connecting the second module at an instant of 0.3 Sec is shown in Fig. 8. The PV current is changed from 5.76A with the first module, into 11.3A with both modules as depicted in Fig. 8a. Whereas in Fig. 8b, the PV voltage is being fixed at the corresponding value of the voltage at MPP from the practical PV curves of modules in Fig. 7a and Fig. 7b at nearly 17.5 V. It has a small overshoot at the instant of power change equals 2V. Furthermore, the power of PV modules is stepped from

103 W to 190 W as shown in Fig. 8c. Figure 8d clarifies that the capacitor voltage is increased from 69 V into 80 V due to the action of the controller to keep the converter operating at MPP of the two modules. After the peak power from the two modules is achieved, it will be passed into the RL load. The current peak value of the phase is changed from 1.3A into 1.6A as shown in Fig. 8e. It is clear from Fig. 8 that the current reaches its steady state after about 14 msec. Also, the voltage has a dynamic fast response and reach its steady state after about 11 msec. Under this algorithm, the tracker gets its MPP value with a fast response about 14 msec. Based on [24] the minimum time 275 msec is required to reach the MPP, Therefore, the proposed algorithm is about nineteen times faster than the traditional algorithm.

From the simulation results, the step change in the phase current is small because the power only change is about 80 %; this power will be divided between the three phases; the output voltage is variable with power change.

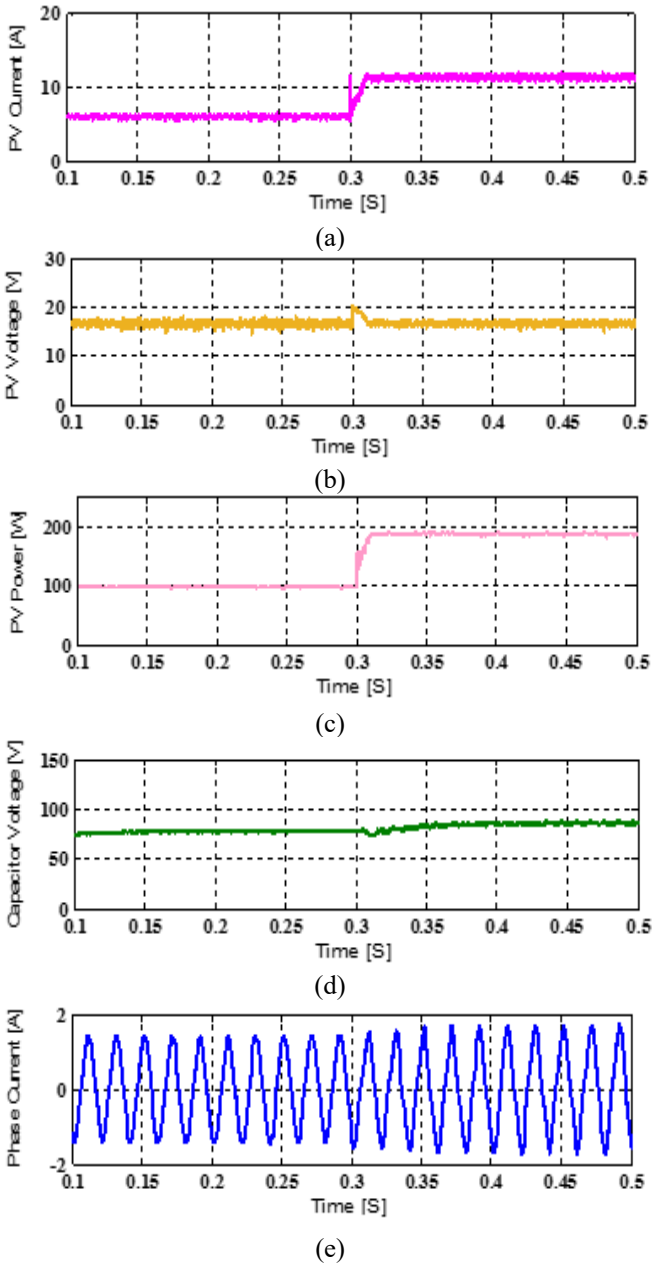

Fig. 8: Simulation results of the system at the power change.

The switching state of the inverter switches has to be updated every sampling time according to minimization of the cost function. The zoomed view for pulsated DC link voltage of qZSI where its value equals zero during the shoot-through case fastens the updating time of the switching signals as shown in Fig. 9.

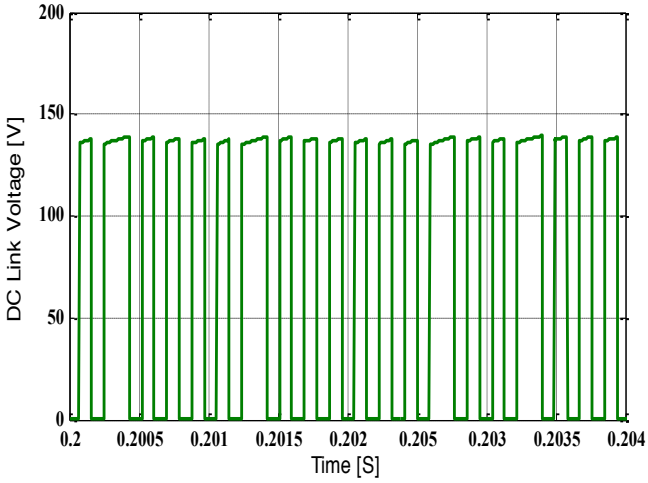

Fig. 9: Zoomed view for pulsated DC link voltage before inverting stage.

5. Experimental Discussion

The proposed controller is validated also by the experimental setup of qZSI and PV system. The testbench is has been built with the same simulation parameters as shown in Fig. 10. The digital code for the experimental implementation of the controller was done based on Digital Signal Processor (DSP) TMS320F28335. The code is fastly done by using the MATLAB/SIMULINK Embedded Coder feature for simplifying the application of the control. Unlike conventional PWM control schemes; there is no requirement to use an external hardware circuit to merge the shoot-through state with the other traditional states. This proves the effectiveness of simplicity of FCS-MPC. The Intelligent Power Module (IPM) is used as an inverter stage with part No. PM50CLA120 IGBT. The module is connected with L-Series IPM Interface Circuit BP7B.

Figure 11 indicates the experimental results for the phase current, capacitor voltage, and the waves of PV modules such as power, voltage, and current. The peak phase current is stepped up from 1.2 A into roughly 1.45 A with connecting the second module. While the input current delivered from PV is stepped from 5.6 A into 11 A. The total power is changed from 100 W into 185 W. There is a slight difference in the experimented power compared with the simulated one due to the assumption of the idealty for the switches and diodes used.

The system is also tested at disconnecting the second module of PV and the experimental results are shown in Fig. 12. The steady state of the system with the first PV module is shown

in Fig. 13, where the frequency of the phase current is 50 Hz and its peak value equals 1.2 A.

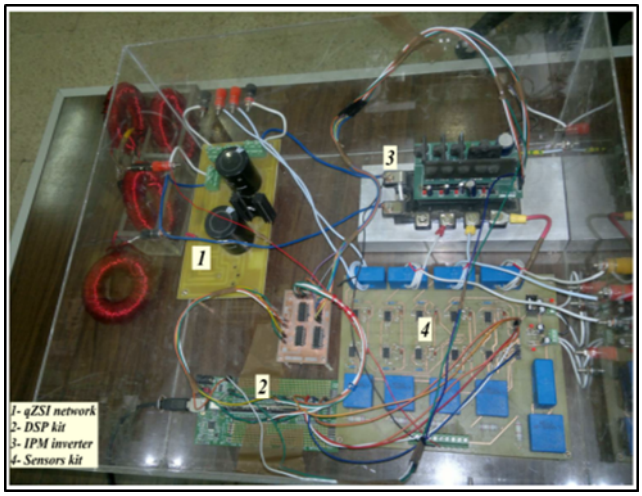

Fig. 10: Experimental setup of the system.

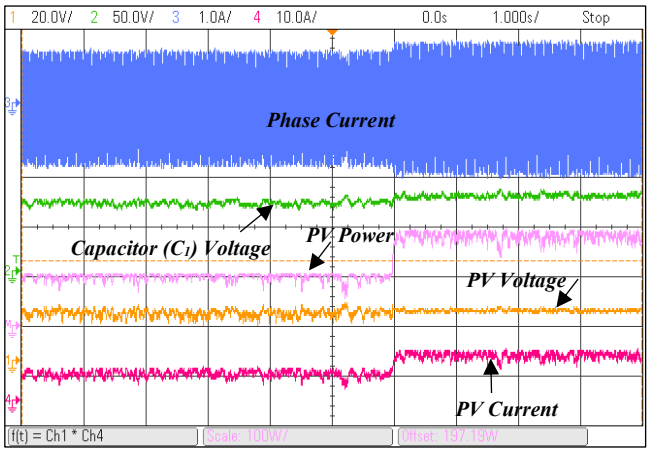

Fig. 11: Experimental results at connecting the second module, from top to bottom: phase current, capacitor voltage, PV power, voltage, and current of PV module.

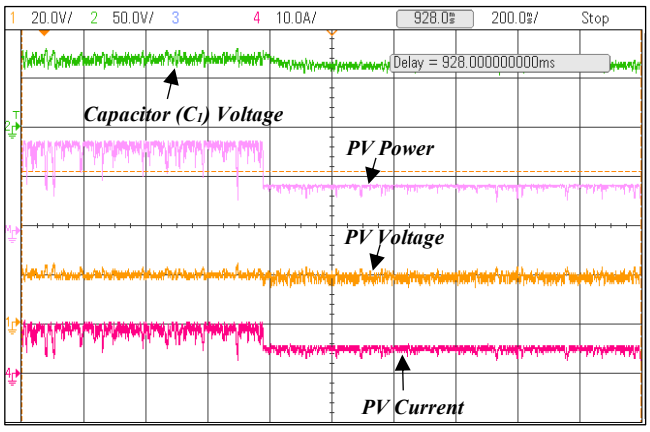

Fig. 12: Experimental results at disconnecting the second module, from top to bottom: capacitor voltage PV power, voltage, and current of PV module.

The DC link voltage again proves the period for applying the sampling time as shown in Fig. 14. The phase current has a distortion waveform due to the lower switching frequency roughly 2 kHz.

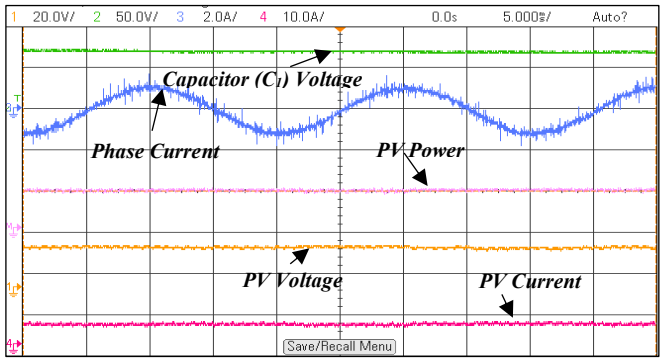

Fig. 13: Experimental results at steady state operation with only the first module from top to bottom: capacitor voltage, phase load current, PV power, voltage, and current of PV module.

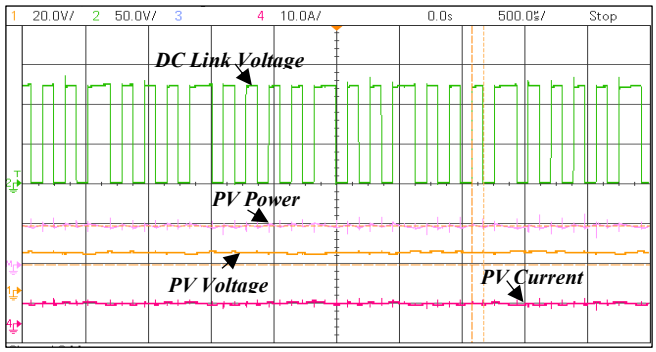

Fig. 14: Experimental results, from top to bottom: pulsated voltage of DC link, PV power, PV voltage, and PV current.

6. Conclusion

The paper introduced detailed theoretical modelling for using FCS-MPC to extract and tracking the maximum power from the system of PV modules with qZSI topology. The tested topology has the buck and boost functionality. The proposed algorithm is being able to extract the maximum power despite the step change in the number of the connected modules. The proposed algorithm controller has high performance in tracking the maximum power of the PV modules. The simulation results are introduced to prove the theoretical calculations. Besides, the viability study of the proposed system is validated experimentally using F28335 digital board.

Acknowledgements

This work is funded in part by the Egyptian Science and Technology Development Funds (STDF) and German Academic Exchange Service (DAAD) under German Egyptian Mobility Program For Scientific Exchange and Excellence Development (GE-SEED) ID: 30290. Any

opinions, findings, and conclusions or recommendations expressed in this material are those of the author(s) and do not necessarily reflect the views of the funding agencies.

References

[1] Z. Peng, W. Yang, X. Weidong, and L. Wenyuan, "Reliability evaluation of grid-connected photovoltaic power systems," IEEE Transaction on Sustainable Energy, vol. 3, no. 3, pp. 379-389, July 2012.

[2] M. Shen, A. Joseph, J. Wang, F. Z. Peng and D. J. Adams, "Comparison of Traditional Inverters and Z -Source Inverter for Fuel Cell Vehicles," in IEEE Transactions on Power Electronics, vol. 22, no. 4, pp. 1453-1463, July 2007.

[3] F. Z. Peng, X. Yuan, X. Fang, and Z. Qian, "Z-source inverter for adjustable speed drives," IEEE Power Electronics Letters, vol. 1, no. 2, pp. 33-35, 2003.

[4] Sham, Noor Mazliza Badrul, Shamsul Aizam Zulkifli, and Ronald Jackson. "An Extend Control Algorithm in PV-ZSI Capacitor-Assisted with Shoot-Through Allowable Boundary on Different Load Cases." International Journal of Renewable Energy Research (IJRER) 8.3 (2018): 1420-1429.

[5] M. Ismeil, M. Orabi, R. Kennel, O. Ellabban and H. Abu-Rub, "Experimental studies on a three phase improved switched Z-source inverter," 2014 IEEE Applied Power Electronics Conference and Exposition - APEC 2014, Fort Worth, TX, 2014, pp. 1248-1254.

[6] M. A. Ismeil, A. Kouzou, R. Kennel, H. Abu-Rub and M. Orabi, "A new switched-inductor quasi-Z-source inverter topology," Power Electronics and Motion Control Conference (EPE/PEMC), 2012 15th International, Novi Sad, 2012

[7]Li, Y., Peng, F. Z., Cintron-Rivera, J. G., & Jiang, S.. "Controller design for quasi-Z-source inverter in photovoltaic systems." 2010 IEEE Energy Conversion Congress and Exposition. IEEE, 2010.

[8] Y. P. Siwakoti, F. Z. Peng, F. Blaabjerge, P. C. Loh, G. E. Town, and S. Yang, "Impedance-Source Networks for Electric Power Conversion Part II: Review of Control and Modulation Techniques," IEEE Transaction on Power Electronics, vol. 30, no. 4, pp. 1887-1906, 2015.

[9] M. Narimani, B. Wu, V. Yaramasu, Z. Cheng, and N. R. Zargari, "Finite Control-Set Model Predictive Control (FCS-MPC) of Nested Neutral Point Clamped (NNPC) Converter," IEEE Transaction on Power Electronics, vol. 30, no. 12, pp. 7262-7269, 2015.

[10] J. Bocker, B. Freudenberge, A. The, and S. Dieckerhoff, "Experimental Comparison of Model Predictive Control and Cascaded Control of the Modular Multilevel Converter," IEEE Transaction on Power Electronics, vol. 30, no. 1, pp. 422-430, 2015.

[11] A. Bakeer, M. A. Ismeil and M. Orabi, "A Powerful Finite Control Set-Model Predictive Control Algorithm for Quasi Z-Source Inverter," in IEEE Transactions on Industrial Informatics, vol. 12, no. 4, pp. 1371-1379, Aug. 2016.

[12] S. Alireza, D. A. Khaburi, and R. Kennel, "An Improved FCS–MPC Algorithm for an Induction Motor With an Imposed Optimized Weighting Factor," IEEE Transaction on Power Electronics, vol. 27, no. 3, pp. 1540-1551, 2012.

[13] M. Wei, A. Loh Poh Chiang and B. Frede, "Maximum power point tracking technique implementation of Z-source inverter through finite step model predictive control strategy," 2012 7th IEEE Conference on Industrial Electronics and Applications (ICIEA), Singapore, 2012, pp. 1523-1528.

[14] A. Ayad, and R. Kennel, "Model predictive controller for grid-connected photovoltaic based on quasi-Z-source inverter," 2013 IEEE International Symposium on Sensorless Control for Electrical Drives and Predictive Control of Electrical Drives and Power Electronics (SLED/PRECEDE). IEEE, 2013.

[15] S. Sajadian, and A. Reza , "Model Predictive Based Maximum Power Point Tracking for Grid-tied Photovoltaic Applications Using a Z-Source Inverter." IEEE Transactions on Power Electronics, Nov. 2016, pp. 7611 - 7620

[16] B. Subudhi and R. Pradhan, "A Comparative Study on Maximum Power Point Tracking Techniques for Photovoltaic Power Systems," IEEE Transaction on Sustainable Energy, vol. 4, no. 1, pp. 89-98, 2013.

[17] M. Ben Smida and A. Sakly, "A Comparative Study of Different MPPT Methods for Grid-Connected Partially Shaded Photovoltaic Systems," Int. J. Renew. Energy Res., vol. 6, no. 3, pp. 1082–1090, 2016.

[18] B. Veerasamy, W. Kitagawa, and T. Takeshita, "MPPT Method for PV Modules Using Current Control-Based Partial Shading Detection," 3rd Int.Conf. Renew. Energy Res. Appl. ICRERA 2014, pp. 359–364, 2014.

[19] B. Ahmad, W. Martinez, and J. Kyyra, "Performance Analysis of A Transformerless Solar Inverter with Modified PWM," 2017 6th Int. Conf. Renew. Energy Res. Appl. ICRERA 2017, pp. 1024–1029, 2017.

[20] Y. Mahmoud, "Toward a Long-Term Evaluation of MPPT Techniques in PV Systems," 2017 6th Int. Conf. Renew. Energy Res. Appl. ICRERA 2017, pp. 1106–1113, 2017.

[21] H. Nademi, Z. Soghomonian, and L. Norum, "A Robust Predictive MPPT Strategy: An Enabler for Improving The Photovoltaic Conversion Source," 2017 6th Int. Conf. Renew. Energy Res. Appl. ICRERA 2017, pp. 1086–1091, 2017.

[22] S. Vazquez, J. I. Leon, L. G. Franquelo, J. Rodriguez, H. A. Young, A. Marquez, and P. Zanchetta, "Model Predictive Control: A Review of Its Applications in Power Electronics," IEEE Industrial Electronics Magazine, vol. 8, no. 1, pp. 16-31, 2014.

[23] P. Cortes, S. Kouro, B. L. Rocca, R. Vargas, J. Rodriguez, J. I. Leon, S. Varquez, and L. G. Franquelo, "Guidelines for Weighting Factors Design in Model Predictive Control of Power Converters and Drives," in proc. IEEE International Conference on Industrial Technology (ICIT), pp. 1-7, 2009.

[24] Soon, Tey Kok, and Saad Mekhilef. "A fast-converging MPPT technique for photovoltaic system under fast-varying solar irradiation and load resistance." IEEE transactions on industrial informatics 11.1 (2014): 176-186.